

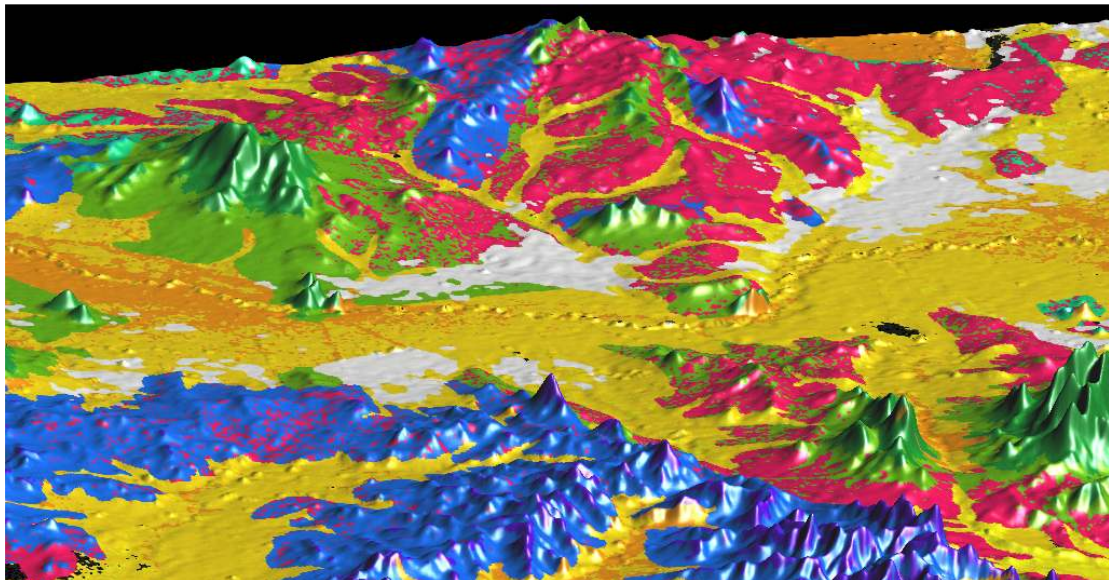


Australian Government
Bureau of Rural Sciences

**Defining sources and stores of salt at Billabong Ck, N.S.W,
using airborne gamma-radiometric and electro-magnetic data.**

P.N Bierwirth

March, 2006



© Commonwealth of Australia 2005

This work is copyright. Apart from any use as permitted under the Copyright Act 1968, no part may be reproduced by any process without prior written permission from the Commonwealth available from the Department of Communications, Information Technology and the Arts. Requests and inquiries concerning reproduction and rights should be addressed to the Commonwealth Copyright Administration, Intellectual Property Branch, Department of Communications, Information Technology and the Arts, GPO Box 2154, Canberra ACT 2601 or at <http://www.dcita.gov.au/cca>.

The Australian Government acting through the Bureau of Rural Sciences has exercised due care and skill in the preparation and compilation of the information and data set out in this publication. Notwithstanding, the Bureau of Rural Sciences, its employees and advisers disclaim all liability, including liability for negligence, for any loss, damage, injury, expense or cost incurred by any person as a result of accessing, using or relying upon any of the information or data set out in this publication to the maximum extent permitted by law.

Postal			address:
Bureau	of	Rural	Sciences
GPO		Box	858
Canberra ACT 2601			

Email: salesbrs@brs.gov.au

Internet: <http://www.brs.gov.au>

Copies available from:
<http://www.brs.gov.au/publications>

Cover Figure: Three-dimensional perspective of aeolian salt sources (red) and surface salt (white) over geology units draped on a DEM, Billabong Ck, N.S.W. The sources and stores of salt have been defined by GIS modelling of gamma-ray and electromagnetic remote sensing data.

Summary

Analysis of airborne geophysical data suggests that Billabong Ck is a key area in understanding salt sources in the Murray Darling Basin. Borehole data indicates that airborne gamma-ray signatures can be used to model upland salt sources in covering sediments while the airborne electromagnetic (AEM) data defines these salt sources as well as salt pathways and accumulations.

The combined modelling and analysis of AEM and gamma-ray data provides a better understanding of salinity in relation to geological materials in the landscape. Although the AEM is expensive and limited in extent, the wide coverage and availability of gamma-ray data makes it possible to attempt modelling of regional salt sources to provide valuable contextual information.

Further, an upland landscape salt model, based on radiometric potassium (K) and thorium (Th) actually correlates with the uppermost AEM layers. The difference is that the gamma model is detecting the source materials while the AEM shows the actual salt, including accumulations in the landscape.

At Billabong Ck, spatial and vertical correlations of AEM data with down-hole data, both conductivity and EC 1:5, suggest that the uppermost layer (0-5m) actually represents 20-25m, meaning that the top 20m of the landscape is not represented. This significantly changes the original interpretations and the data needs to be recalibrated to produce the missing data.

New analysis of the AEM data shows that salt sources in the cover overlying saprolite are distinguished from areas of salt accumulation lower in the landscape. The deeper salt accumulation at Kangaroo Ck is actually several zones separated at depth and linked to discrete source areas. These salt zones appear to flow into a salt layer at 30-40m that is continuous along Billabong Ck linking to the Walbundrie Sump.

The source areas of saline sediments covering saprolite in upland areas are localised and generally have a low-potassium (K) and mid-range thorium (Th) airborne radiometric signature. Strong evidence suggests that areas with this signature have a high component of salt-bearing aeolian material, derived from deflationary events in the Murray Basin. These aeolian dust deposits appear to be a localised source of salt at Billabong Ck and this is likely to apply generally in the Murray-Darling Basin (MDB).

Introduction

Aim

The MDBC Airborne Geophysics Project was set up to demonstrate the usefulness of airborne geophysics for the management of salinity at a catchment scale. This was to be achieved by providing substantial airborne geophysical coverage, and on-ground calibration of the airborne data, for areas with perceived salinity problems. The Billabong Ck data was investigated (Jones et al, 2003) but this was early in the overall project (when BRS had a limited image analysis capability) and was relatively brief

with little analysis of the gamma-radiometrics data. The aim of this report was to further investigate the airborne electro-magnetic (AEM) data and the gamma-radiometrics with respect to salinity, soils and land management.

Previous BRS report

The initial Billabong Creek study was part of the MDBBC Airborne Geophysics Project that was set up to demonstrate the usefulness of airborne geophysics for the management of salinity at a catchment scale. A drilling program was conducted by BRS (Jones et al, 2003) to provide ground verification for the AEM data. The initial report by Jones et al (2003) provided interpretation and analysis of both data from airborne geophysics and data acquired from the borehole drilling program. The area is situated just to the north of Albury in southern NSW (see Figure 16 in Jones et al, 1993). Figure 1 shows the surface (0-5m) AEM data layer that was provided by Fugro Airborne Surveys Ltd. Major findings of the report were that:

- downhole electrical conductivity primarily related to salt contents
- high salt and conductivity tend to relate to clay and low salt to sandy cover and saprolite
- conductivity is dominated by salt-bearing regolith rather than bedrock
- low conductivity equals low salt
- deeper higher conductivities ($> 15\text{-}20\text{m}$), associated with salt, occur at Kangaroo Ck and to the west of Walbundrie although the latter is not salty at the surface.
- Simmons Ck salinity is generally shallower than 15m

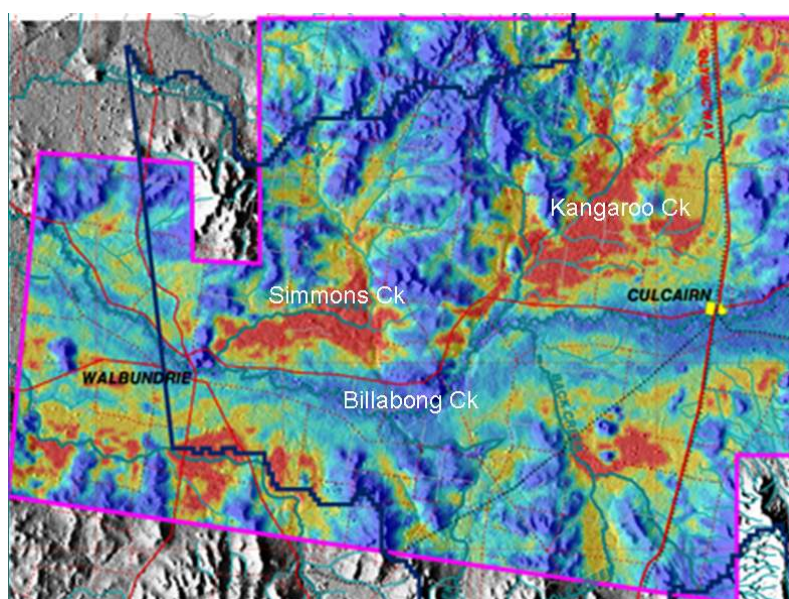


Figure 1. Original surface (0-5m) layer of the AEM data at Billabong Ck. The image is 40km across

In the original study there was little interpretation of the airborne gamma-radiometrics data. This is partly a result of lack of image analysis capability in the BRS at the time. There were comments made about the possibility of extrapolating salt store but no analysis done of the airborne gamma data or the downhole gamma readings. General observations were high element concentrations in bedrock outcrop areas, lower values

on colluvium, variable signatures in alluvium where there were high values relating to active and recent channels.

Jones et al (1993) reports on the results of bore-hole drilling and analysis (see Figure 2 for locations) and provides visual representation of down-hole properties. However 3 of the 20 drillholes (BC9, BC15 and BC20) have not been analysed for EC and soil moisture. Also downhole logs for BC12 are not presented in the report.

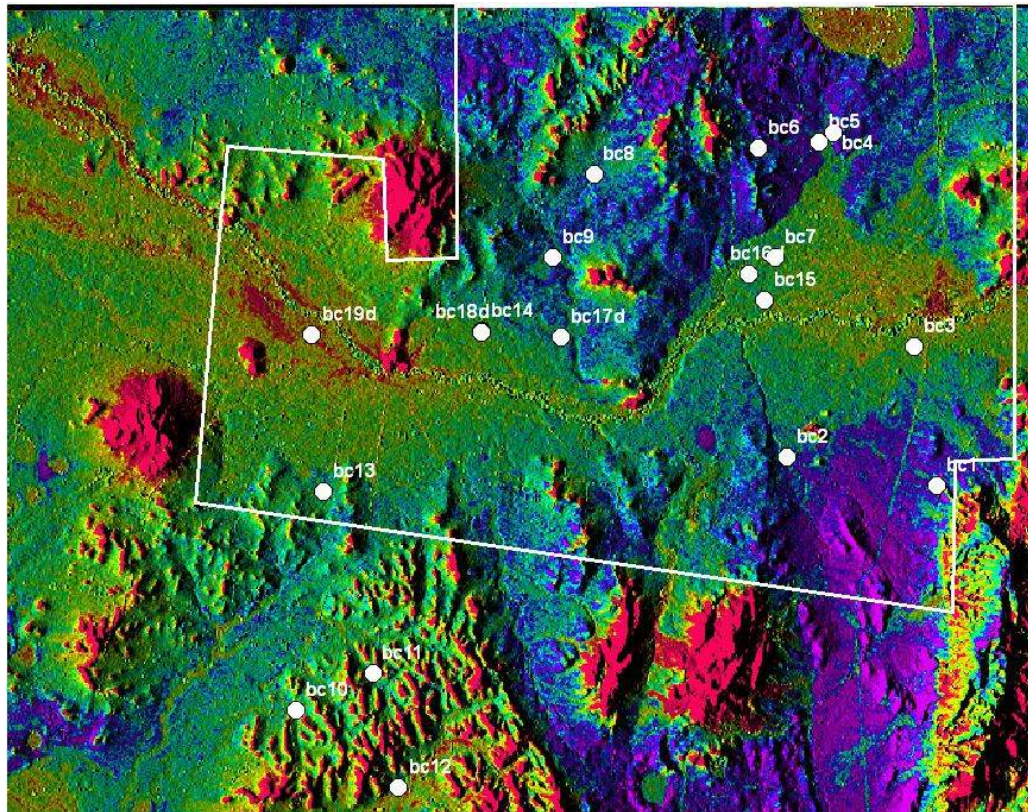


Figure 2. Borehole locations with AEM survey area (white). The image is potassium concentration draped on a DEM.

Another look at the AEM data

Analysis of borehole data

Profile diagrams for analysed borehole information are shown in Jones et al, 2003. In the analysis of geophysical and borehole data it is important to recognise the different elements of the basement geology, regolith materials and groundwater. In simple terms, the boreholes can be separated into upland profiles and lower alluvials. In the upland case, locally derived colluvial cover overlies weathered saprolite (bedrock material) whereas the lower alluvials are transported materials sometimes also overlying saprolite at depth. This distinction is particularly important for interpreting gamma-radiometrics where colluvial and alluvial signatures are very different.

Relationships between salt (EC 1:5) and downhole conductivity

As discussed in the earlier report, there is a good correlation between salt (as measured by EC 1:5) and downhole conductivity, although in general there was brief analysis done. The interpretation was that high conductivity is related to salt and moisture in clay-silt units. Regression coefficients in one alluvial hole (BC7) suggested that variations in EC 1:5 ($R^2 = 0.67$) explained most of the variation in down-hole conductivity but that clay was a significant factor ($R^2 = 0.40$). The report also stated that saprolite sequences tended to have low conductivities except for volcanic units. Borehole BC6 was used as an example of low conductivity in the cover and saprolite. Re-examination of the borehole data shows that the cover in this hole actually has high conductivity and that generally low conductivity in the saprolite is true but only below the upper 15m. Figure 3 gives down-hole conductivity versus effective salt content for 25m of covering sediments and 21 metres of granite saprolite for BC5. The positive relationship between salt and conductivity is split into two populations for saprolite (100% clay-silt) and cover (75% clay-silt). This shows that an increase in clay content by 33% can add 200mS/m to conductivity values.

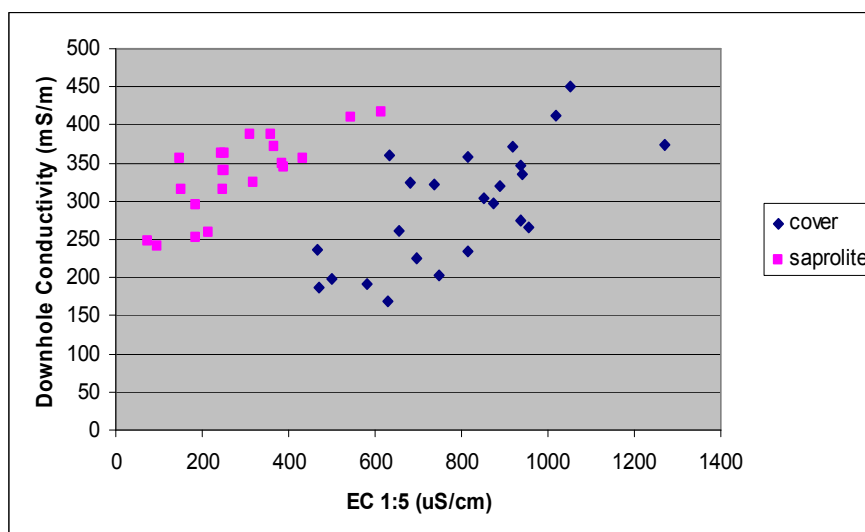


Figure 3. Relationship of EC 1:5 to downhole conductivity in borehole BC5 for granite saprolite and overlying cover.

The same relationship appears to generally apply for different holes (Figure 4). The cover material in BC5 and the alluvial sediments in both BC3 (55% clay-silt) and BC7 (76% clay-silt) contain significant sandy materials resulting in data values closer to the “salt” line on Figure 4. In contrast, the saprolite in BC5 and the sediments in BC6 (82 clay-silt) and BC16 (85 clay-silt) are more clay rich. Similarly variations in the conductivity in the colluvial cover in BC10, which contains low salt, appear relate to clay variations. Another aspect that could be important is that BC5 and other holes, that have cover overlying granite saprolite, can have relatively low conductivity corresponding to high salinity. This may be due to the component of residual granite materials in the cover in these areas.

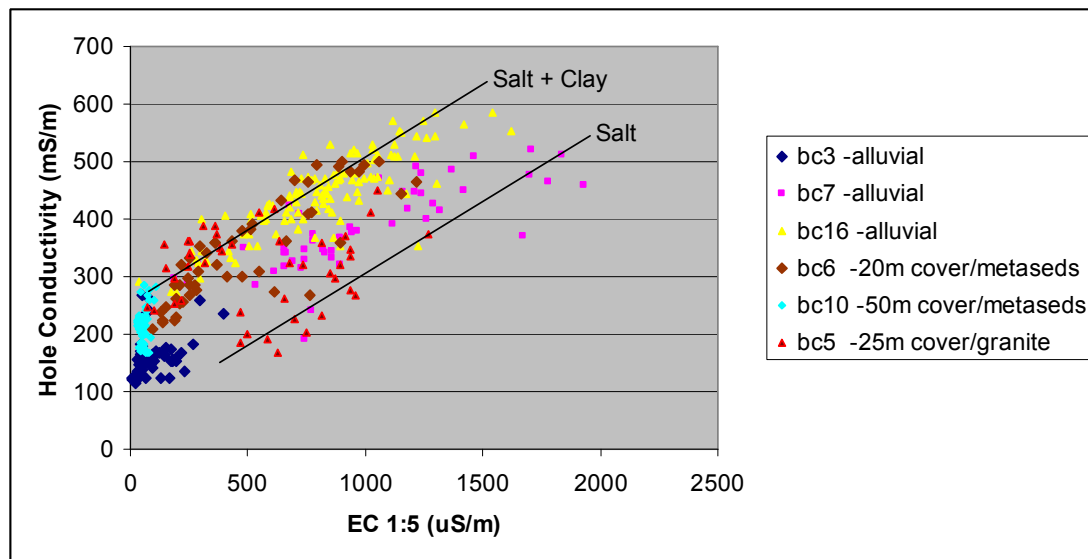


Figure 4. Relationship of EC 1:5 to downhole conductivity in borehole BC5 for granite saprolite and overlying cover

Analysis of Airborne EM (AEM) data

For many AEM surveys, the airborne depth conductivity layers provided by the contractor have been recalibrated based on modelling and calibration to borehole/ground conductivity (Lane et al, 2004). For the Billabong Ck area this has apparently not been done. Figure 5 shows AEM pixel values for the depth slices compared with averaged down-hole conductivity and EC 1:5 for the same intervals in BC7. While there is a good relationship between EC 1:5 and conductivity, the AEM values do not relate well showing a pronounced reduction toward greater depths. This is presumably related to the assumption of zero conductivity at depth that is used in AEM processing. This situation is present in all holes.

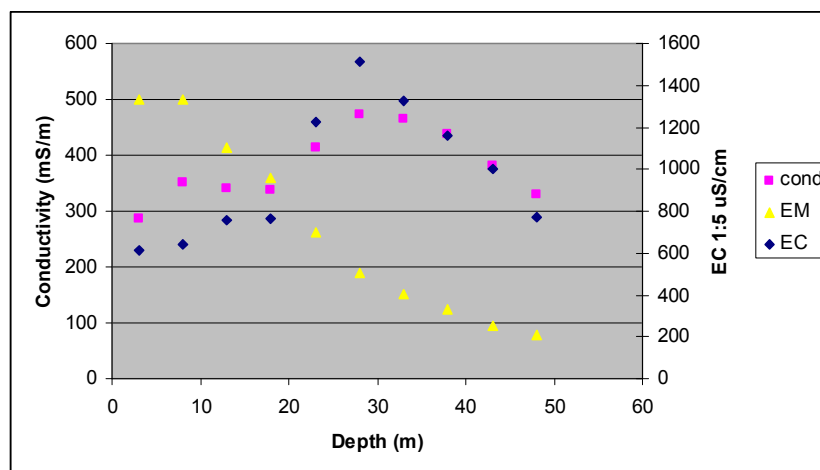


Figure 5. Comparison of downhole conductivity and EC 1:5 with airborne EM for borehole BC7.

Spatial relationships between all boreholes in depth layers for the top 30m (Figure 6) show a good correlation between salt (EC 1:5) and down-hole conductivity but there is a generally poor relationship between salt and the AEM data in the top 20m layers.

This latter relationship improves with depth but the AEM has an increasing offset to lower values.

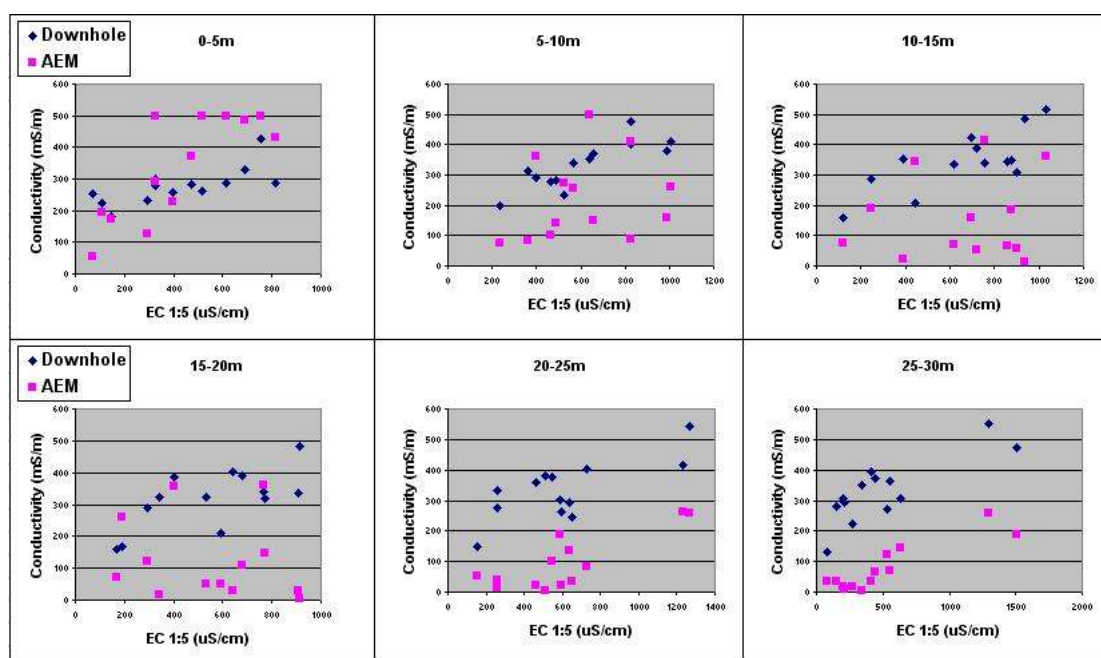


Figure 6. Spatial correlations between EC 1:5 and conductivity for all available borehole data in the top six depth layers. Magenta values are the supplied AEM data.

This poor relationship between salt and AEM is investigated further by analysing the correlation between specific AEM layers and down-hole properties for every layer below (Figure 7). This was done in the light of other AEM studies where the data had to be effectively “dropped down” (St George study - Lane et al, 2004). Figures 7a and 7b show that the surface EM layers (0-25m) are actually correlated with the conductivities and EC’s respectively of the layer that is about 15-30 m below. This equating depth appears to reduce for the lower layers. The average depth offsets were 25m for conductivity and 20m for EC 1:5. This is evidence that the AEM data is displaced in the vertical dimension relative to the actual landscape.

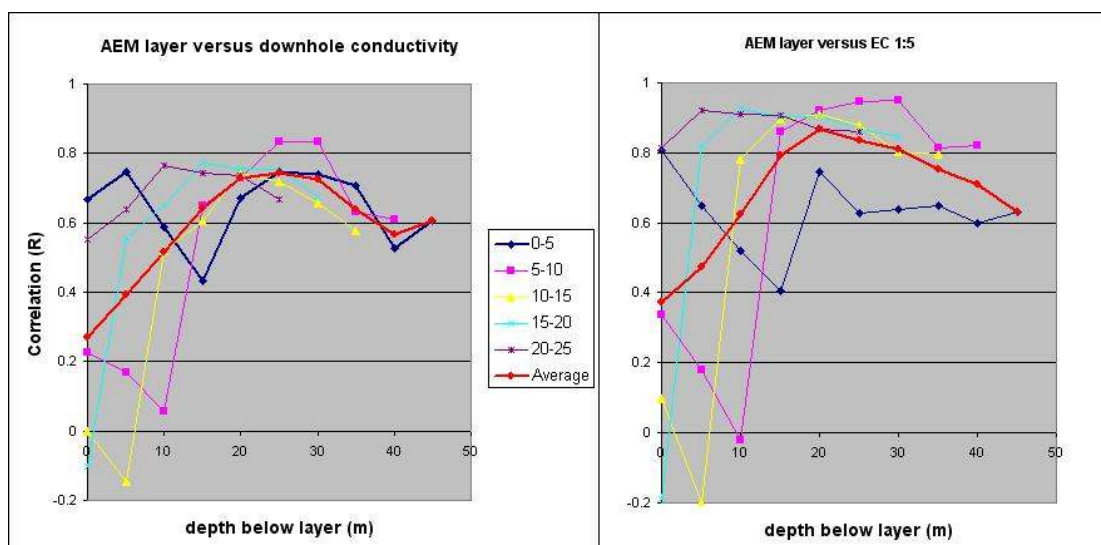


Figure 7. Correlation of AEM layers to down-hole conductivity and EC 1:5 in underlying layers.

Further evidence for the vertical AEM errors is shown in Figure 8 where correlation graphs are displayed for the new AEM layers moved to 20 metres below the original depths. Much better correlations are now observed for all layers. The offset in values at greater depths is also reduced. This shows that the AEM was originally poorly calibrated in two dimensions at least, i.e. vertically displaced together with the gradual decline in values at depth (shown in Figure 5). Also since the highest AEM layer equates to the landscape at about 20m depth, the surface layers are effectively missing.

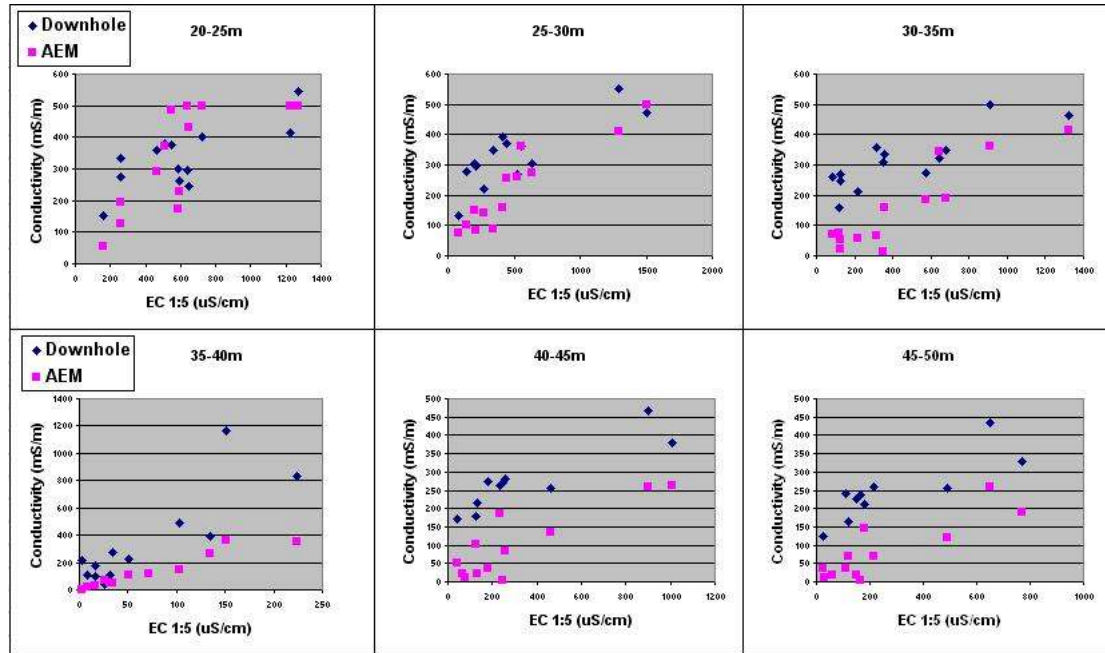


Figure 8. Spatial correlations between EC 1:5 and conductivity for all available borehole data after shifting the top six depth layers down. Magenta values are the supplied AEM data.

The data shown in Figure 8 can be used to produce estimated EC 1:5 data from the AEM data. For each layer, linear relationships were found to transform the AEM data. Figure 9 shows representative slices the AEM data calibrated to EC 1:5. The depth of each layer has been shifted down by 20m and the layers shown correspond to those presented in Jones et al (2003 - Figures 7-10). In comparison there are much higher relative salinities at depth.

The image shown in Figure 9(d) is similar to Figure 10 in Jones et al (2003) although the colours are reversed for better visualisation of the shallow salt areas shown in red. With more subtle image enhancement, the deeper salt stores in the Kangaroo Ck alluvial terrace can be clearly seen to be segmented and apparently connected to more shallow salt stores that are overlying saprolite. This appears to indicate that the deep extensive salt stores at Kangaroo Ck are sourced locally which has implications for management. In general the spatial extent, of salt-affected landscape, increases toward the surface. Given that the top 20 metres is effectively missing from the AEM data, this extent is expected to be larger at the surface. This has particular significance for the interpretation of radiometrics

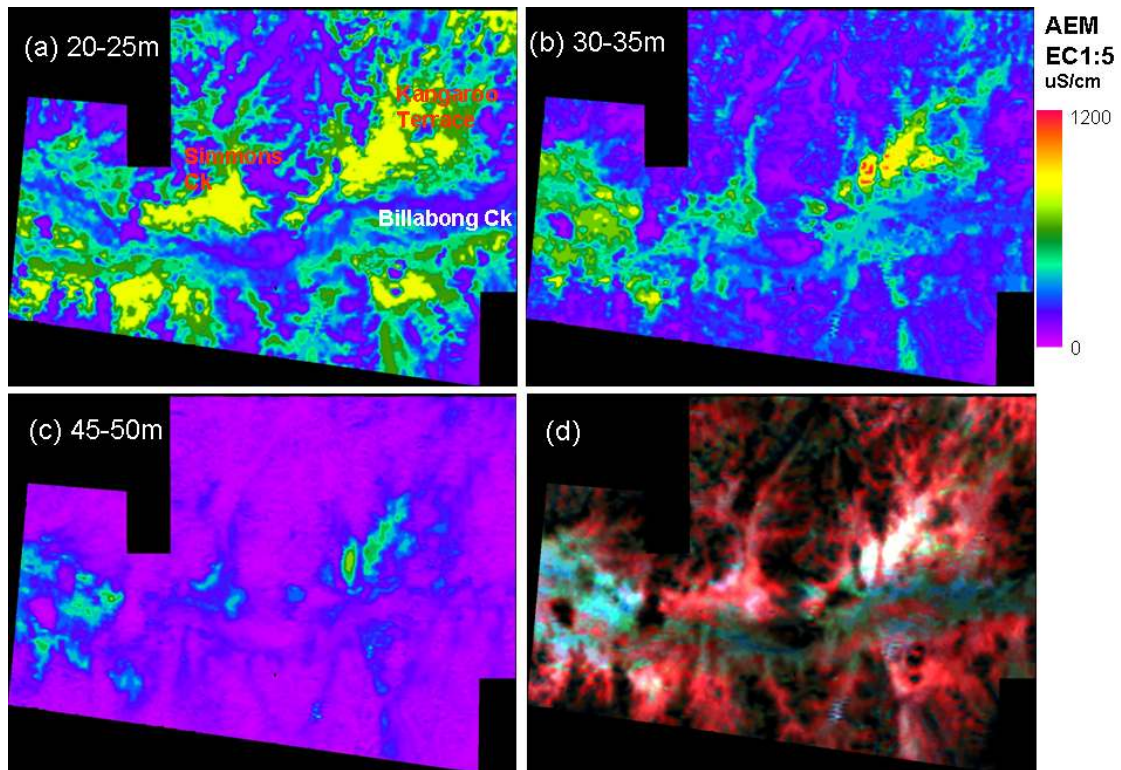


Figure 9. (a)-(c) AEM data downward-shifted by 20m and calibrated to EC (d) composite of AEM depths 20-25m, 35- 40m, 45-50m as RGB respectively.

Another way of viewing AEM data in a single plan view is to perform a Principal Components Analysis (PCA) transformation on the multi-layer data (Figure 10). Typically PC 1 displays features that are correlated in all layers. Subsequent PCs as displayed in Figure 10 show the variations in the landscape. Blue areas represent the shallow salt stores generally overlying saprolite at approximately 25-40m depth. Red areas are similar but more saline and deeper, sometimes suggesting pathways. Green, cyan and white areas represent high salinity from surface to depth generally in alluvial systems while cyan and white areas are the highest salinities at depth (> 70m). Pink areas are close to current day drainage and represent low salt throughout the profile possibly due to flushing and deep drainage from the river systems

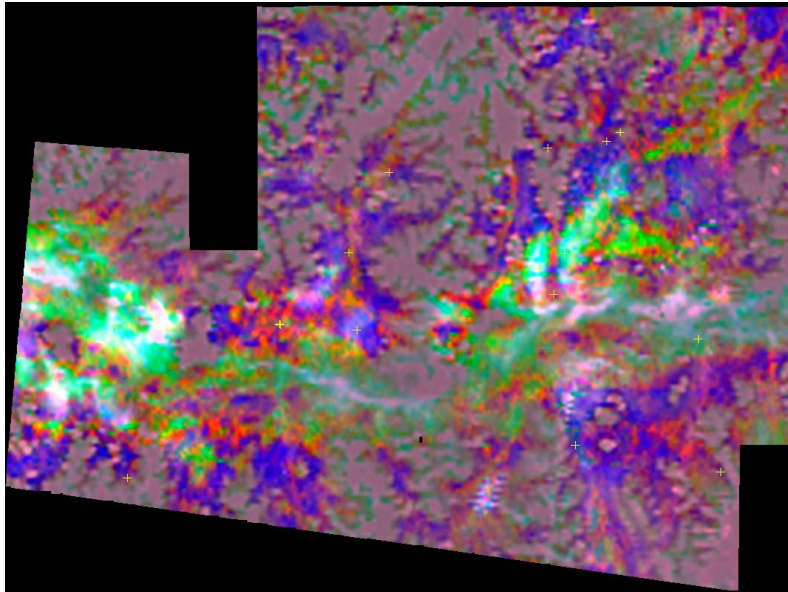


Figure 10. Principal Components Analysis (PCA) of the upper 10 AEM depth layers. PC 2,3 and 4 are shown as green, blue and red respectively.

Airborne gamma radiometrics

Background on gamma radiometrics

Airborne gamma-spectrometry (AGS) uses raw wavelength data to derive abundances of the major gamma-emitting elements potassium (K), thorium (Th) and uranium (U). This provides spatial images of the geochemistry of the upper (approximately 30-45 cm) rock/soil layer. However element concentrations at the surface can often be related to subsurface properties (Bierwirth, 1986).

Source minerals for Potassium (K) are feldspars and mica's and their weathering products such as illite clays. Uranium (U) and Thorium (Th) are present in significant quantities in accessory minerals. The spatial distribution within the landscape of K, U and Th and the decay products of U and Th are also a function of physical and chemical weathering processes as well as sediment transport processes. In terms of weathering, K is by far the more mobile of the elements, Th is more resistant to weathering and U is perhaps less well understood. U image data is also often noisy due to low counts collected by airborne sensors. Image interpretation depends therefore on the primary mineral content and the weathering patterns of these minerals influenced by the geomorphology.

Previous studies in relation to salinity

In a detailed study of radiometrics at Kyeamba Creek near Wagga Wagga (Bierwirth, 1996), a relationship was observed between salinity discharge zones and low K areas (Figure 11a). This area is contained within Ordovician metasediment geology where high K relates to bedrock signatures of the shallow lithosols. At the time it was thought that the low K was associated with areas of clay related to increased salt. Soil samples largely from the upper landscape showed a relationship between K and salt (EC 1:5) in the soil profile.

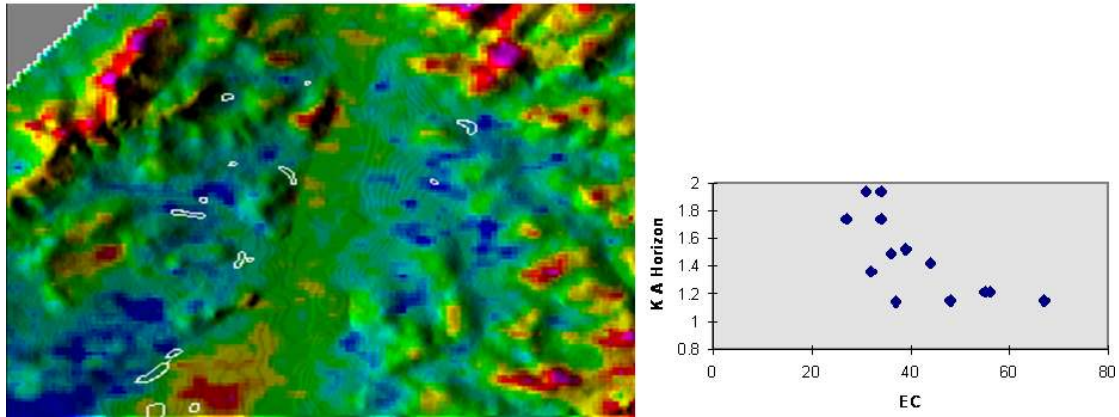


Figure 11. (a) Image of K draped on a shaded DEM at Kyeamba Ck, NSW. The white outlines are salt scalds and the image is 7 km across. (b) soil sample measurements of total K in the A horizon expressed as percent versus EC 1:5 (uS/cm) from the B horizon.

Detailed soil sampling also showed that, in the metasediments landscape, lower K is associated with increased weathering and depths of colluvium (Figure 12). The initial assumption was that the very low K areas were an extension of this phenomenon but as discussed next these areas may be a result of introduced Aeolian materials.

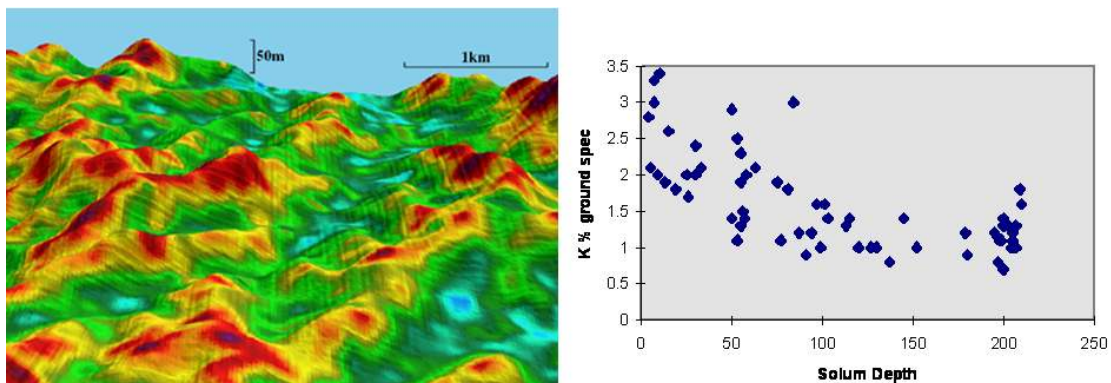


Figure 12. (a) 3-D perspective of K draped on a DEM for upland areas east of Kyeamba Ck, NSW (b) solum depths (depth to saprolite) compared with K ground spectrometer measurements.

Following on from this work and based in the same organisation, Wilford et al, 2001 attempted to relate low K to salt storage at Bethungra, NSW. Although a loose relationship between landscape K and stream salinity was presented, they noted that low K related to areas of clays and intense bedrock-weathering and that these were residual landscapes likely to contain a significant component of Aeolian materials.

Landscape salt sources in Aeolian materials

It is widely accepted that salts have been introduced to the landscape rather than being derived from bedrock sources (Evans, 1998). It has been postulated that salt accompanying dust derived from deflationary events in the Murray basin is the source of salts found in the uplands region of the Murray-Darling Basin (Bowler, 1983)

At Simmons Creek within the current study area of the Billabong Creek catchment, English et al (2002) suggest that significant salt storage relates to Aeolian parna deposits. These reworked aeolian deposits now blanket the topographically low parts of the catchment and correspond with low gamma-responses. Even in the present-day climate, saline dust-fall (dry particulate grains of resuspended terrestrial dust with some entrained salt sourced substantially from salt lakes and dune-fields in the Mallee and western Riverine Plain) and dissolved salts in rainfall (principally sourced from the ocean) can be considerable. Modern dust may contain up to 50% by weight of salts.

In the same area, McKenzie and Gallant (2005) used airborne gamma K and topographic indices to map soil classes associated with Aeolian materials. They concluded that units dominated by Aeolian materials were associated with low K and slopes less than 6 degrees

Analysis of Airborne Gamma Radiometrics data

Interpretation of image data

For the interpretation of gamma-ray radiometric data, the understanding of geology is fundamental since mineral components are a major source of gamma-rays. Geological units, taken from the NSW geological survey 1:250,000 mapping, are shown in Figure 13. The area consists of Ordovician metasediments (Os - phyllite, slate), Silurian igneous rocks (granites and volcanics) and Devonian sediments (Dls) that include sandstone, conglomerate, siltstone and shale.

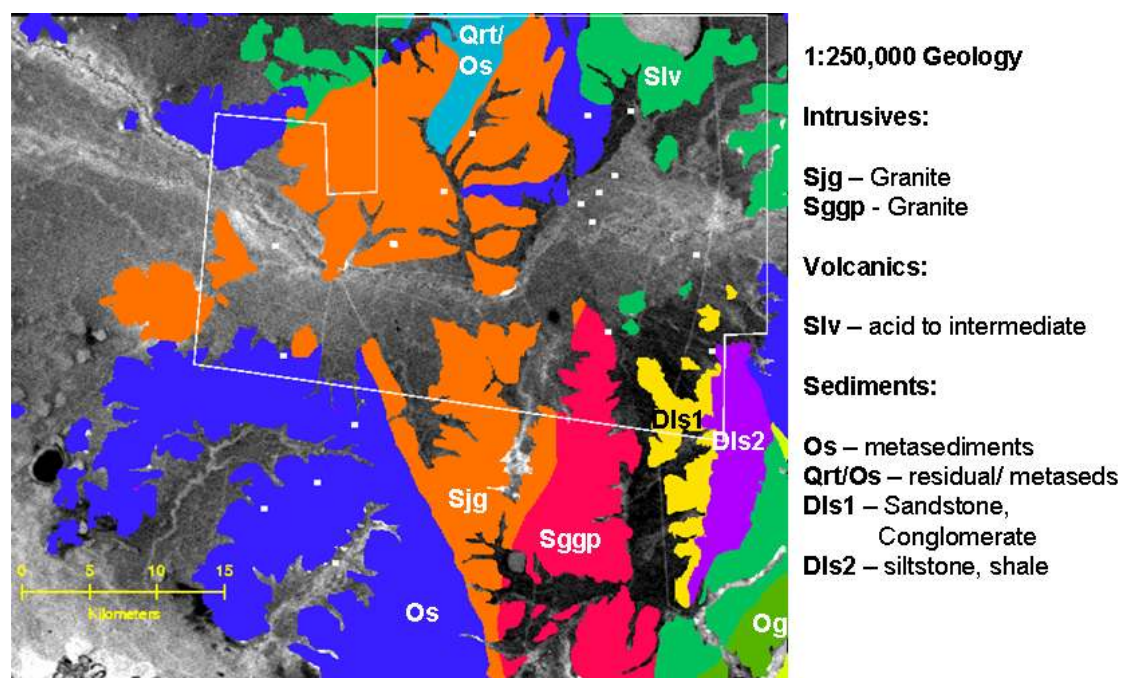


Figure 13. Geology of the radiometrics survey area. The AEM survey area is shown as white and the potassium image is shown in grey tones in areas mapped as alluvial cover.

The original interpretation of the gamma radiometrics data was based on a ternary image where the three elements are combined as RGB (Jones et al, 1983). The

associations of the individual elements are clearer when also viewing individual element images (Figure 14a-d). As reported by Jones et al (1983), there are commonly high gamma element values where the bedrock is shallow for most rock-types (cf Figure 13). Exceptions occur for some granites (a in Figure 14a), which have low Thorium, and quartz sandstones (b) that are low in all elements. In-situ and weathered colluvial soils typically have lower element concentrations such as those associated with the metasediments (c). Importantly, significant parts of these data appear to be dominated by wind-blown transported materials that overly the bedrock-derived materials. One of the most striking features are the low K areas (d), north of Billabong Ck, where significant aeolian components have been mapped (English et al, 2002; McKenzie and Gallant, 2005; English et al, 2002). This area also has a moderate Th concentration which is the classic signature for Aeolian materials (Bierwirth et al, 1996; Dickson and Scott, 1998). The proximity of this material to the major salt zones, shown by the airborne EM in Figures 9 and 10, at Simmons Ck and Kangaroo Ck, also adds weight to the hypothesis that the Aeolian materials represent the major salt sources in the area.

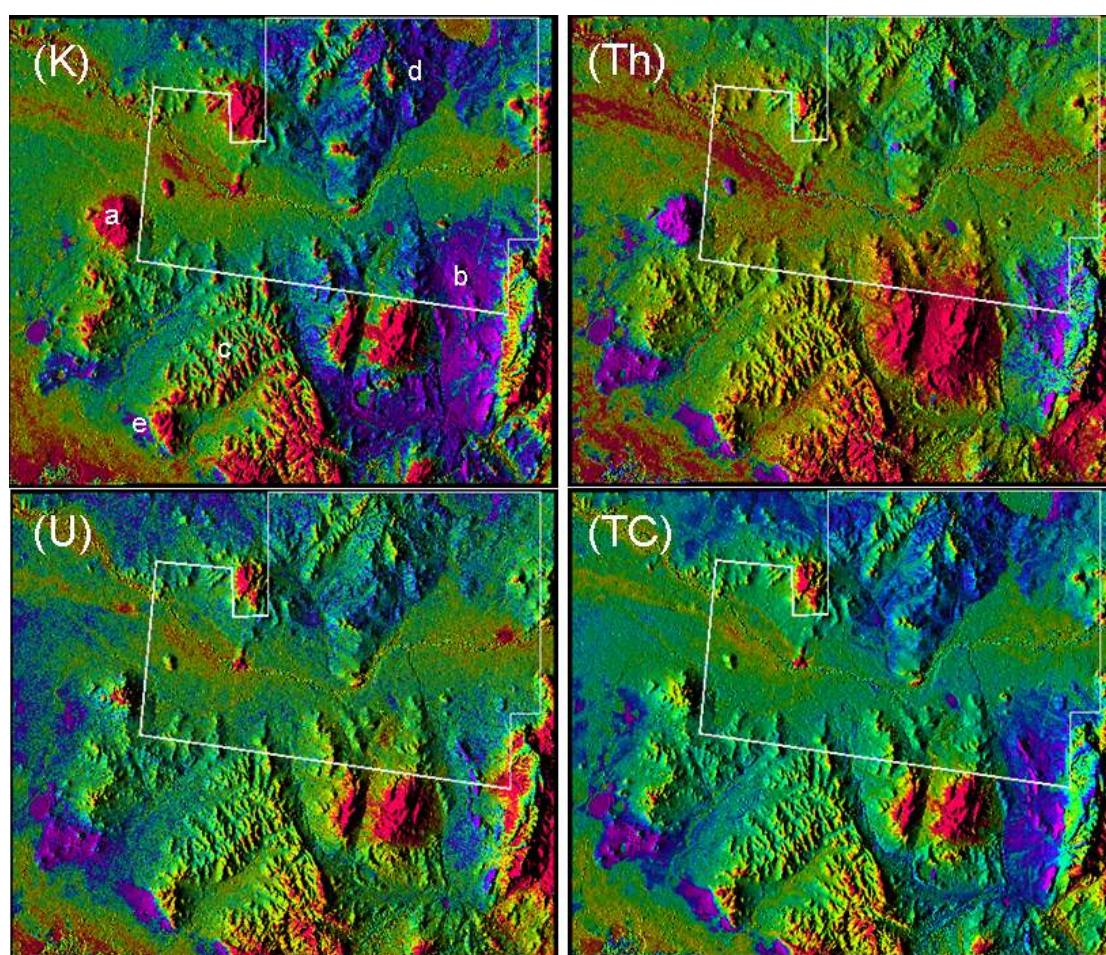


Figure 14. Airborne gamma-ray radiometrics images (a) potassium (b) thorium (c) uranium and (d) total count. Colours are relative values (red – highest, through yellow, green, blue to magenta-lowest). The white outline is the extent of the AEM data.

Alluvial systems have higher gamma element signatures with the highest values generally relating to active deposition of silts and the lowest values relating to both

clays and older weathered (particularly for K) sediments. Other interesting features are the low element values (e) that appear to relate to lunette sands that are part of an ancient lacustrine environment in the south-west of the area

With an understanding of geology and geomorphic processes, together with field checking, the gamma radiometrics data can provide important information about landscape materials.

Analysis of borehole data

The above interpretation of the surface gamma signatures indicates that the down-hole gamma-ray measurements will vary depending on materials related to location in the landscape. Unfortunately the down-hole gamma readings are only total count (TC) and while there are broad correlations between TC and the individual elements, this data is not adequate for any calibration exercise of multi-element airborne gamma data. Nevertheless the analysis of down-hole data does provide important information about the regolith materials (Figure 15). A plot of down-hole gamma-rays versus EC 1:5 for selected holes (Figure 15a) shows 3 distinct groupings:

- 1) Alluvial (BC1 and BC7) where low to medium total counts have variable EC's. Hence, in alluvial sediments, the image data is unlikely to be a useful indicator of salt storage.
- 2) Low-salt colluvial soils over metasediments south of Billabong Ck (BC10 and BC11). Gamma values above 120 cps are generally saprolite.
- 3) High-salt cover over variable geology (BC5, BC6 and BC8). The pattern for these three holes is similar except for part of BC8 where higher gamma values with EC 1:5 (soil extract) between 600 and 1200 $\mu\text{S}/\text{cm}$ are found just above the base of the cover and in the top of the saprolite. This may possibly relate to a residual surface or relict alluvial clay zone that has become salty.

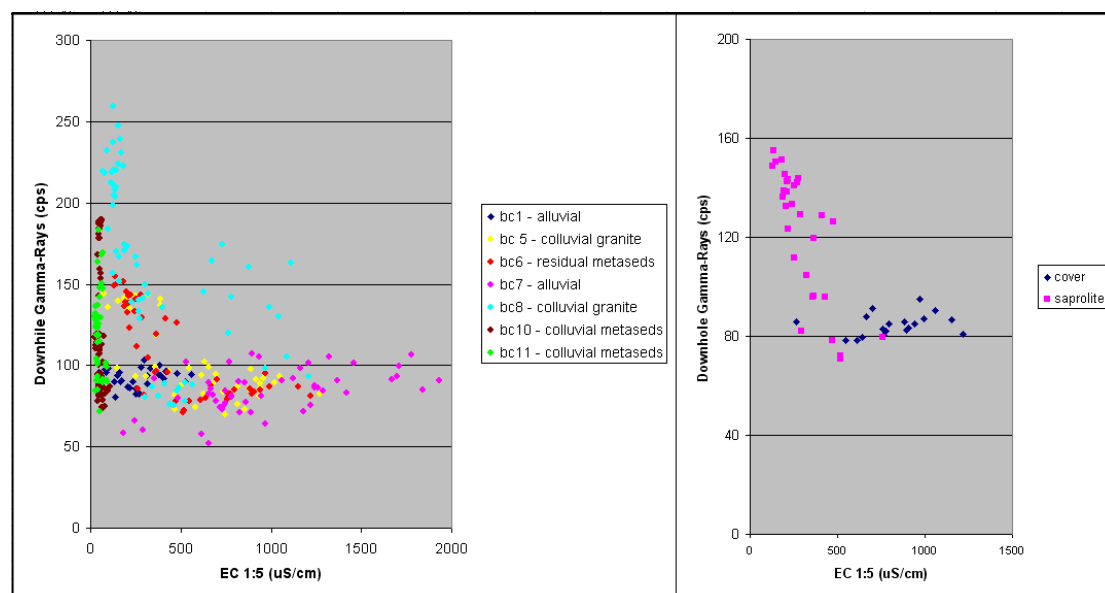


Figure 15. Relationship between downhole gamma-ray total count with salt (EC 1:5) soil-extract for (a) various types of holes and (b) cover versus saprolite in BC6.

The third category describes boreholes, north of Billabong Ck, that have salt in both covering sediments and upper-saprolite. Deeper into the saprolite, as the bedrock

material becomes less weathered, the gamma counts increase and the salt content declines (Figure 15b). BC6 from this group has a considerably different profile to that of BC10 and BC11 despite having the same underlying geology. This evidence supports the idea that boreholes BC5, BC6 and BC8 are influenced by saline aeolian materials, as mapped by McKenzie and Gallant, 2005, that have been deposited across different geological units.

Further evidence for the presence of Aeolian materials is the analysis of grainsize. Two diamond drillholes, BC17 and BC18 were analysed in the original Billabong Ck study (Jones et al, 2003) using laser analysis. One of these, BC17 (see Figure 2), is also in the third category described above having 14 metres of saline cover sediments overlying granite saprolite. The results of laser grainsize analysis for BC17 are shown in Figure 16. In contrast to BC18, which is in alluvial sediments, there is a second grainsize peak in the range 0.0078 – 0.0156 mm and these are fine silt sized particles. This is equivalent to 6-7 Phi and, significantly, this relates to the mean grainsize for modern day dust (6.6 - 6.8 Phi) (Melis and Acworth, 2001).

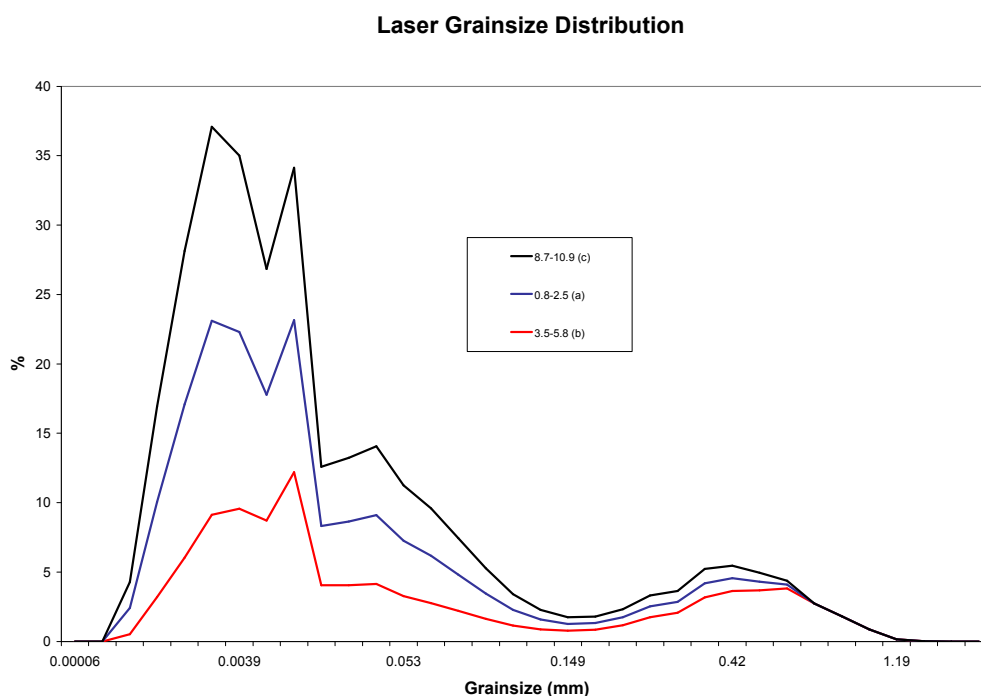


Figure 16. Laser grainsize analysis of covering sediments in borehole BC 17d. From Jones et al, 2003.

If these areas of Aeolian materials are major sources of salt as the AEM data suggests, how can these areas be spatially characterised? Presumably the AEM can detect salt at the surface and would be able to detect salt bearing Aeolian materials as well as areas of accumulation. However in this survey area the surface 20m or so is missing and areas of windblown materials are likely to be more extensive than shown by the 20m depth layer. AEM data sets also tend to be limited in extent, focussing on the salinity outbreak areas rather than the regions of source sediments.

Given earlier evidence for low K associations with salt in upland areas (Bierwirth, 1996), the relationship between all gamma-emitting elements and borehole salinity was investigated in the Billabong Ck area. Unfortunately no individual element concentration data was collected by the down-hole geophysics so that only the airborne data could be analysed and the comparison with borehole data has limitations since an airborne footprint is about 100m in diameter. From the borehole log data, a number of holes were selected as being upland where a relationship between airborne radiometrics and salinity might occur. This is because lowland, i.e. alluvial, areas often have accumulated salts sourced from upland areas, as shown in Figures 9 and 10, so that relationships between salt and salt-source materials (detected by radiometrics) are less likely. The selection of upland boreholes was based on the Multi-Resolution Valley Bottom Flatness (MRVBF) index (Gallant and Dowling, 2003) which is derived from topographic modelling and an index of MRVBF < 2.7 was used to define erosional uplands (McKenzie and Gallant, 2005). Pixel values, for these holes and for all elements, are shown in Figure 17 compared with the average EC 1:5 for the cover and top 15m of saprolite. This zone of saprolite was included due to the general observations of higher EC 1:5 interpreted to be due to salt infiltration of the weathered bedrock. Pixel values are presented for both the nearest value and averaged values upslope (for 1km using elevation contours) from the borehole site. A broad negative relationship is observed for both K and Th and this had been expected (particularly for K) based on the earlier observations. The airborne U data is less clear and this could be due to the large errors introduced from low-count noise that is commonly a problem for this element.

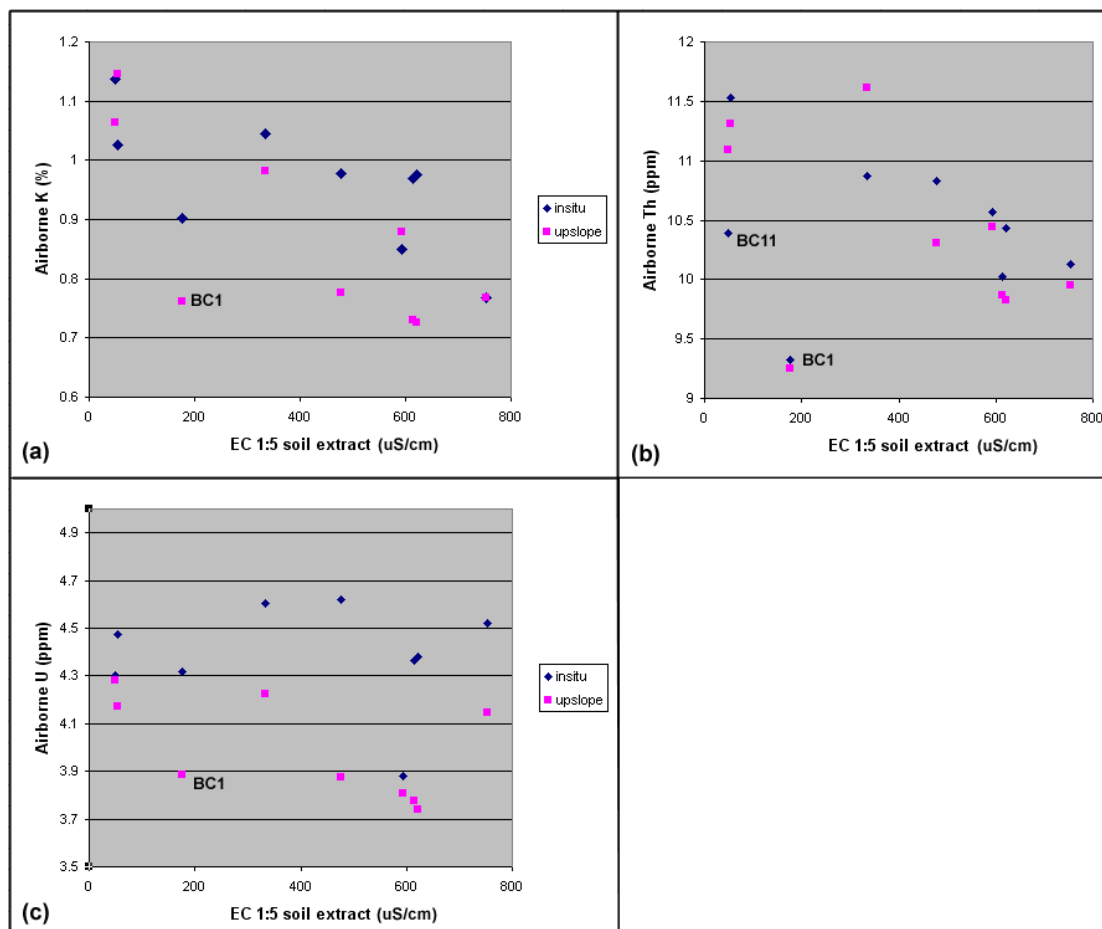


Figure 17. (a) Airborne K pixels values for boreholes determined by a topographic index (MRVBF) to be in colluvial cover over saprolite versus the average EC 1:5 for the cover including the top 15m of saprolite. These are presented for both the nearest value and averaged values upslope from the borehole (b) same for airborne Th (c) same for airborne U.

Errors are introduced to this correlation of airborne data with down-hole readings, due to differences in measurement area and also in some cases by the presence of shallow alluvial cover that is often expressed by elevated element concentrations (e.g. bc4 and bc5 in Figure 18). Also some of the salt in boreholes are likely to be related to source materials that are upslope from the site. To overcome this, regions of interest were drawn to include the area, based on the DEM, that would roughly incorporate up-slope colluvial sediments from with a maximum distance of 1km. Within these areas, the interpreted surface alluvials were excluded and the average K concentration was calculated. These upslope values of K corresponding to each hole can be compared with insitu values (Figure 17). The relationship is generally improved and the results indicate that upland salt storages can broadly be estimated using the airborne K and Th data. Some deviation can be explained by geology. For example, BC 1 (Figure 17a and b) is in a foot-slope area of quartz-sandstone hills and has a correspondingly low K value (similar to saline aeolian soils) for the upslope area that relates to low K sandstone outcrops. The same site has a low Th value relating to the quartz sand content, and this is much lower than the Aeolian saline soils. With this information, it appears possible to derive an index from K and Th that might separate low-salinity sandy soils from highly-saline Aeolian soils. Conversely one site with low salinity in metasediments (BC 11) has a similar Th signature to Aeolian soils but a contrasting K signature.

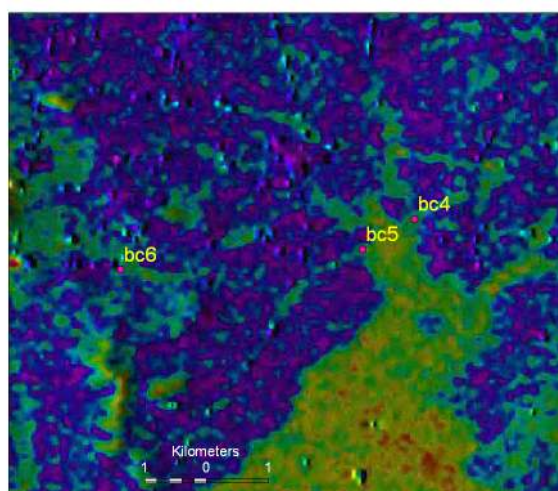


Figure 18. A zoomed in area of the K image showing three boreholes used in the upland analysis

Deriving upland salt store from airborne radiometrics

Landscape characteristics of Aeolian soils

Given the above evidence, it appears that the airborne radiometrics can be used to model the distribution of Aeolian materials, and hence salt sources. The approach

depends on how the introduced Aeolian deposits lie in the landscape in relation to geology and geomorphology. Previous work at Wagga Wagga (Chen, 2001) and at Billabong Ck (McKenzie and Gallant, 2005) indicates that aeolian dust deposits, often red clays, can form a continuous mantle, particularly in high plains. At Wagga Wagga, the Aeolian soils are characterised by a bi-modal pattern in the silt and clay fraction, one mode in course silt (4-6 Phi) and the other in clay. This is similar to sediments at Billabong (BC 17, see Figure 16). In floodplains the red clay is basically absent although Aeolian materials are likely to be present mixed with recent sediments. On hills with average slope >30%, the red clay contains significant amounts (up to >50%) of gravels (i.e. mixed with locally derived colluvium) and exists only at lower and foot-slopes. On hills with average slopes of 10–30%, mixed colluvium/ Aeolian and blanket Aeolian may alternately occur.

Modelling Aeolian dust deposits

As mentioned earlier, McKenzie and Gallant (2005) used a low airborne K threshold and DEM-derived indices to map soil classes, associated with Aeolian materials that are likely to be strongly associated with salt sources. Figure 19 shows the results of their soil model in comparison with the K image. The model incorporates the MRVBF terrain variable, derived from the DEM, which effectively separates alluvial soils from upland areas that contain Aeolian materials. In the upland areas, the Aeolian classes are defined using $K < 111$ counts per second (cps) and slope < 6%. While erosional classes are primarily defined by $K > 111$ cps or slope > 6%.

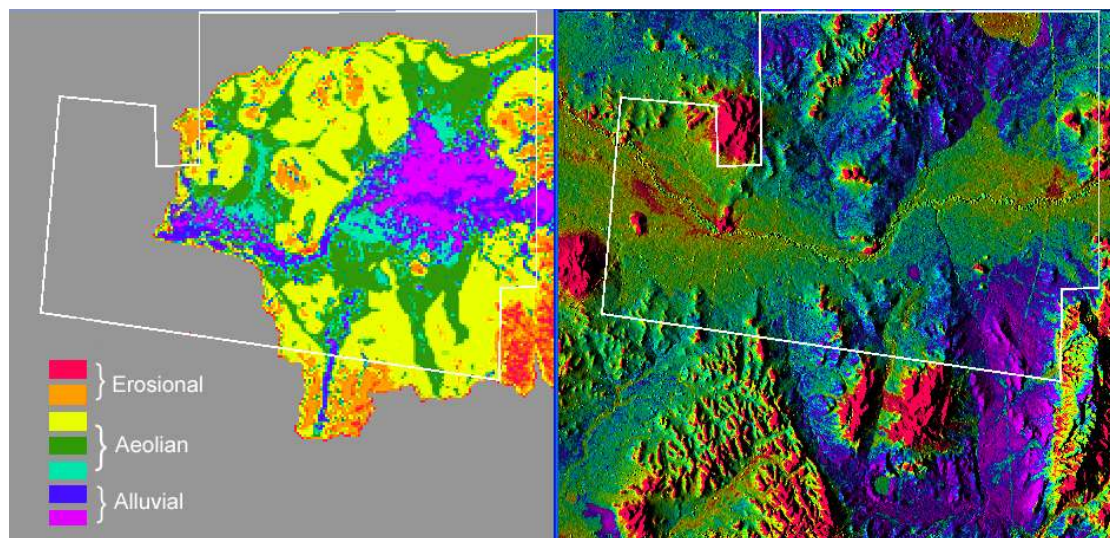


Figure 19. (a) Soil model derived from K and DEM indices (from McKenzie and Gallant, 2005) – spatial resolution is degraded compared to the original data (b) K image draped on the DEM.

Potential problems with the method described above are that:

- geology is not incorporated in the model meaning that colluvial areas with low slopes for low-K lithologies might be interpreted as Aeolian soil. This is apparently the case in the south-east of the area where low-K sandstone colluvial soils are interpreted as Aeolian units.
- the constraint that Aeolian soils only occur in low slope areas assumes that Aeolian materials only occur as a blanket rather than mixed with colluvial material as shown by Chen (2001) at slopes of 10-30 degrees.

- gamma-ray counts depend on the acquisition system, i.e. the size of the crystal and the flying height, and should be calibrated to element concentration.
- lunette soils and other alluvium variations due to source materials will not be detected by classifying alluvial classes on slope alone.

As mentioned above, part of the problem is that Aeolian soils and certain geology types (such as quartz-sandstones in the Billabong Ck area) have overlapping K signatures. The quartz-sandstone erosional areas appear to be well defined as very low thorium values (bottom-right in Figure 14c, see geology unit Dls1 in Figure 13) since quartz sandstones are relatively free of thorium accessory minerals compared to aeolian dust that has moderately high thorium (presumably attached to Fe-oxides). These sandy soils are mis-detected as Aeolian soils by McKenzie and Gallant (2005) (Figure 19a) indicating that the threshold of 6 degrees slope is ineffective at separating colluvial from residual landscapes.

Apart from masking the sandstone areas, the problem can be overcome by incorporating the Thorium data into a potential model. One simple model is achieved by calculating the Euclidean distance (E_D):

$$E_D = \sqrt{(K_i - K_t)^2 + (Th_i - Th_t)^2} \quad (1)$$

Where (K_i Th_i) are the radiometric data values for i^{th} pixel and (K_t Th_t) is the target value for pure saline Aeolian soils. Prior to this calculation, the K data was transformed so that the mean and standard deviation equalled those for the Th data. A target value of 0.7% K and 10ppm Th for saline Aeolian soils were obtained from Figure 17. Using equation 1 above, E_D was calculated and pixel values extracted for upland boreholes (Figure 20). In general there is a much better correlation between ED and upland salinity than for individual elements K and Th. The borehole BC1, that has a similar K response to saline soils, is now separated due to the very low Th concentration for sandy soils.

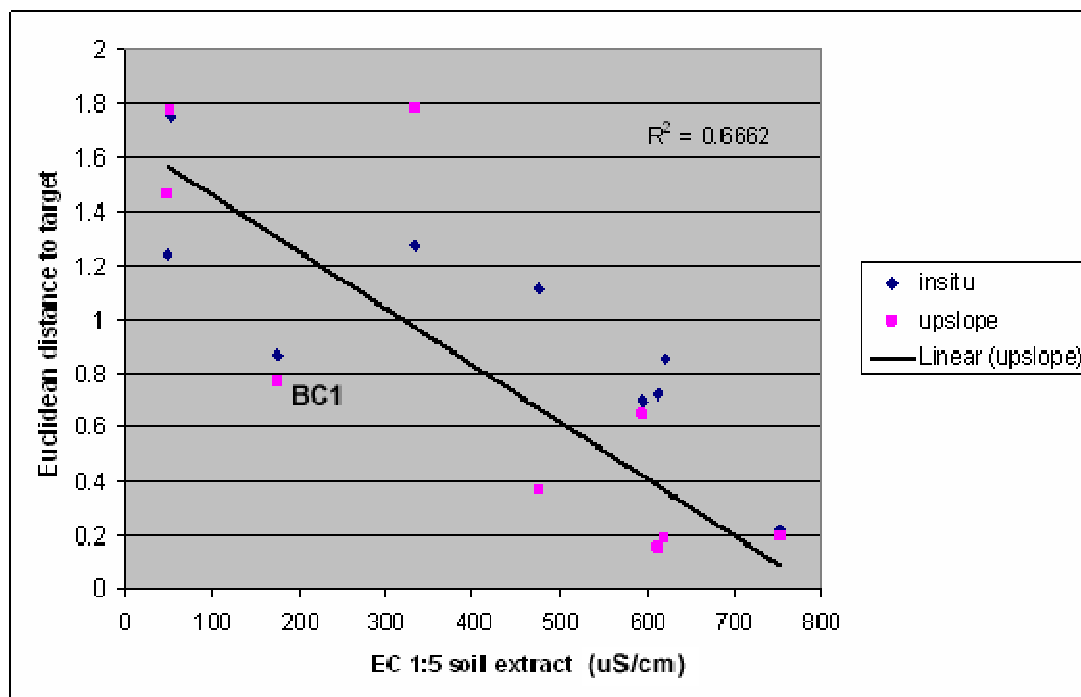


Figure 20. Correlation between EC 1:5 of the soils in upland boreholes to the Euclidean distance from pixel values to a specified target value of K and Th for saline Aeolian soils.

Using the assumed linear relationship between E_D and EC 1:5 from Figure 20, the radiometrics data were calibrated to EC 1:5 of the soil for upland areas (Figure 21). Surface areas of high salt defined by the AEM are also shown on this image and there appears to be a strong relationship between upland salt sources defined by the radiometrics and salt accumulations lower in the landscape. A soil with EC 1: 5 of 700 uS/cm is considered saline with respect to the viability of crops. As a source for salt accumulations lower in the landscape, the value would be less by some degree. It is likely that yellow to red areas (EC 1:5 – 400 to > 700 uS/cm) in Figure 21 are major salt sources in the billabong area.

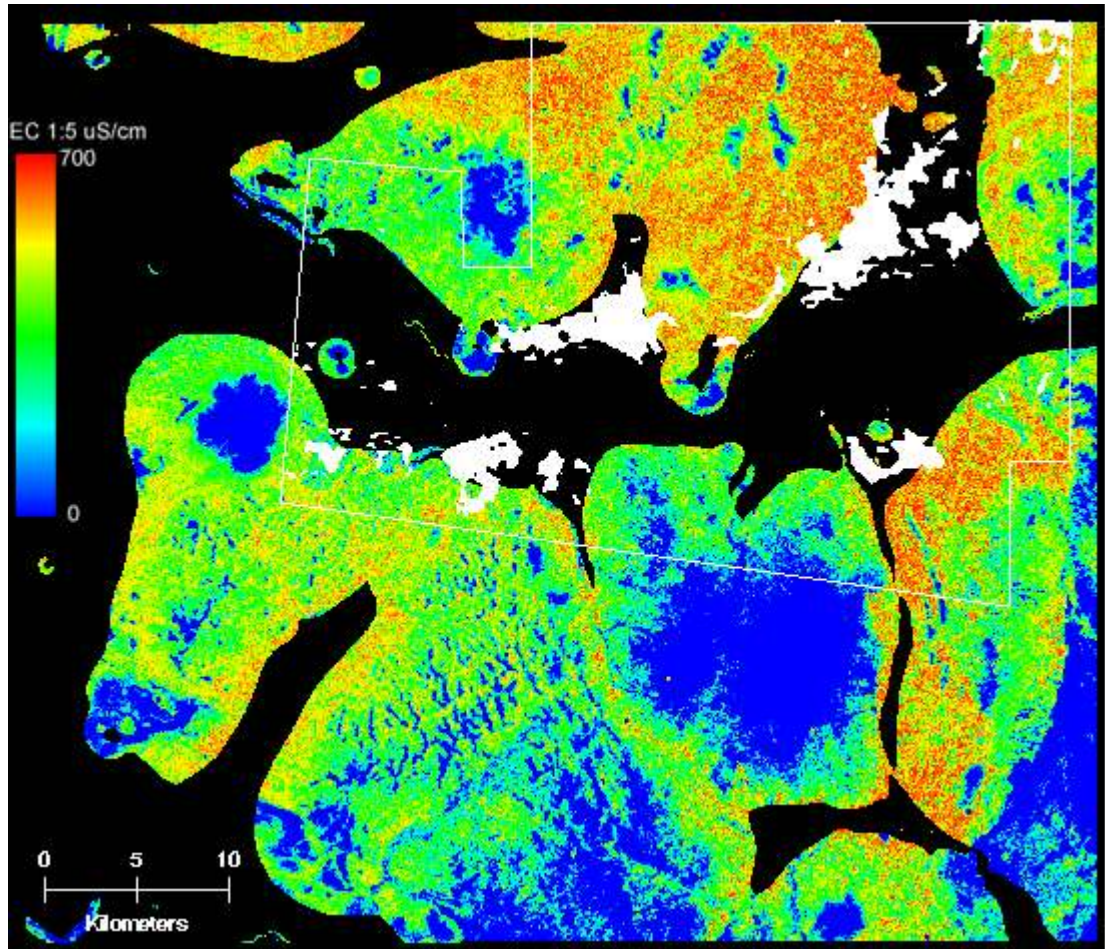


Figure 21. Upland salt model based on Euclidean distance and airborne K and Th calibrated to borehole EC 1:5 data. Black areas are alluvium defined by thresholding the MRVBF topographic index. White areas, indicating salt, are the highest values of uppermost AEM layer (20-25m).

The alluvium was not modelled since:

- radiometric signatures are unlikely to reflect materials to much depth (i.e only the --
- surface layer of multi-layered transported materials)
- aeolian materials are likely to be reworked
- salt accumulations present in the lower landscape may not be attached to their source material

Having said that, it is possible that there are flat areas in the defined alluvium where significant aeolian deposits may occur. Alluvial areas are unmasked in Figure 22(b). There does appear to be areas that may be influenced by Aeolian dust deposits in the mapped alluvial area that are potentially salty. This indicates that the alluvium can also be modelled, particularly in the Billabong Ck area, remembering that in these the modelled source materials do not equate to actual salt accumulation.

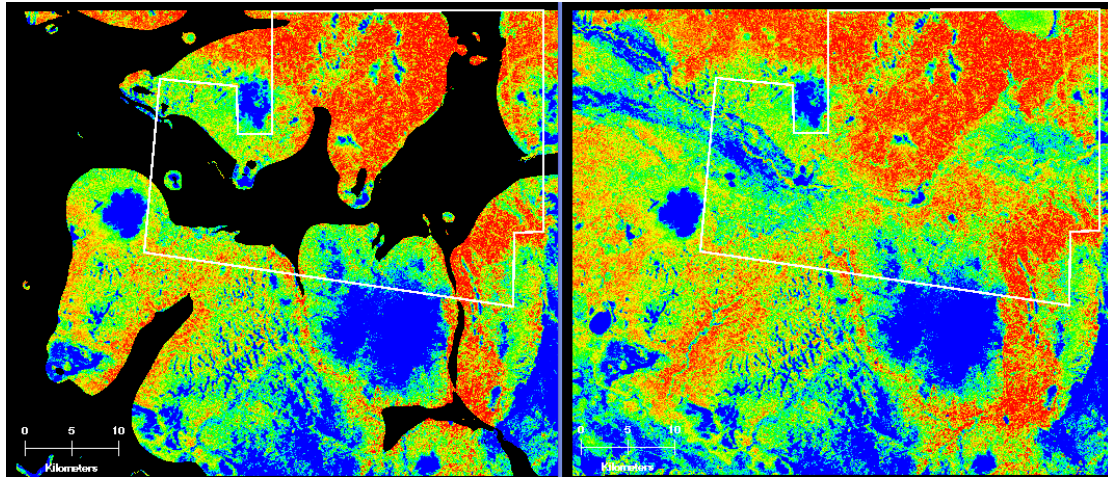


Figure 22. Comparison of (b) Figure 20 and (a) the same model but with alluvium modelled.

If the upland salt model derived from the airborne K data is valid, there should be a reasonable correlation with the calibrated AEM data although the uppermost 20m of the landscape is not represented by the latter. Figure 23 shows the comparison and generally there is a good correlation. The AEM data (Figure 23b) shows similar levels of EC 1:5 to the salt sources defined by the gamma-ray data (Figure 23a). At about 20 metres depth, the AEM indicates increased salt levels adjacent to the floodplain, a feature that would be expected as salts moves down through the landscape. On the other hand, the gamma-radiometrics model shows a more uniform pattern as this relates to more evenly distributed Aeolian salt source materials. Overall, this correlation with the AEM data indicates that the airborne K and Th salt model is highly significant. It becomes particularly important given the extensive coverage and availability of airborne gamma-radiometrics.

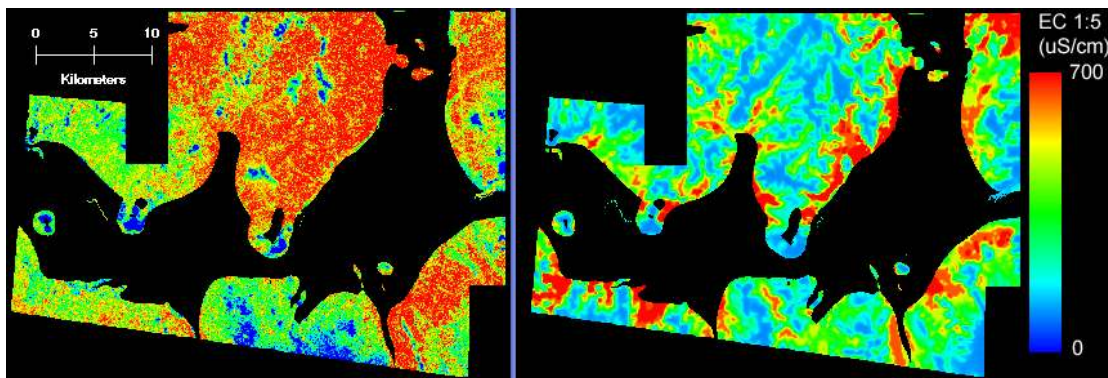


Figure 23. Comparison of calibrated salt models derived from (a) airborne K and (b) the airborne EM.

Conclusions

At Billabong Ck, AEM data is largely correlated with salt although the analysis of borehole data shows separate lines of correlation between EC 1:5 and down-hole conductivity depending on clay content. Without significant variation in salt, AEM data would correlate with clay variations. Several boreholes suggest that relatively low conductivities may be associated with saline cover overlying granite saprolite in upland areas.

Spatial and vertical correlations of AEM data with down-hole data, both conductivity and EC 1:5, suggest that the airborne data at Billabong Ck is poorly calibrated. These data need to be recalibrated by the contractor. However shifting the data down by about 20 m produces a good correlation between AEM conductivity and both down-hole conductivity and EC 1:5. Unfortunately this means that the top 20m of the landscape is not represented. This changes interpretations presented in the original BRS report. For example, the original estimate of 15m of saline cover at Simmons Ck changes to 35m.

Better image enhancement and image processing allows for further understanding of the AEM data. For example, colour composites and Principal Components Analysis (PCA) help to differentiate zones in the landscape. Salt sources in the cover overlying saprolite are distinguished from areas of salt accumulation lower in the landscape. The deeper salt accumulation at Kangaroo Ck is actually several zones separated at depth and linked to discrete source areas. These salt zones appear to flow into a salt layer at a 30-40 that is continuous along Billabong Ck although this layer is not well tested by drilling. The zone appears to link through to the area known as the Walbundrie Sump. In this area a single bore (BC19) shows moderate EC 1:5 down to the base of the upper alluvials at 40m but not the high conductivities and deeper salt that the AEM indicates for the general area.

Saline covering sediments in the north of Billabong Ck have a uniform, relatively low down-hole total count signature. These areas are highly saline compared with low-salt colluvial cover south of Billabong Ck (BC10, 11). This suggests that salt is not everywhere in the cover, but that it is localised. Borehole data at Billabong Ck also show that low-K airborne radiometric signatures in upland areas relate to the high salinity (EC 1:5) of the cover material.

A mounting body of evidence suggests that the low-K saline cover at Billabong Ck contains significant aeolian material, derived from deflationary events in the Murray Basin, and that these deposits are the source of salt in uplands areas of the Murray-Darling Basin (MDB). At Billabong Ck, evidence for Aeolian materials include grainsize analysis and other identification work (McKenzie and Gallant, 2005).

An upland landscape salt source model was generated, based on the K and Th relationship to define the most saline Aeolian classes. A good comparison exists between the uppermost AEM layer (20-25m) and the gamma upland salt model. The radiometrics detect surface elements of Aeolian materials that often appear to relate the salinity of the deeper cover profile. At Billabong the AEM is showing some of these surface elements but also deeper salt accumulations due to water movement whereas the radiometrics Euclidean-distance model is showing the location of aeolian dust salt sources.

As many previous studies have found, the modelling of AEM data can provide detailed information about the location and inferred movement of salt in the landscape. Combined with AEM, the use of gamma-radiometrics enables an understanding of geological materials and potential sources of salt in the upper landscape. Both the AEM and radiometrics data indicate that salt stores and sources

are localised. A knowledge of where the salt is coming from and moving to is fundamental to any management action plan.

Studies in other parts of the MDB have indicated similar relationships between airborne radiometrics and salt sources. Given the relatively wide coverage of these data it is recommended that this modelling be attempted at more regional scales and this could help to put the salt problem into context.

Acknowledgements

The author would like to acknowledge the assistance of Ian Mullen and Peter Baker, both of BRS.

References

Bierwirth, P.N., Gessler, P. and McKane, D. (1996) Empirical investigation of airborne gamma-ray images as an indicator of soil properties - Wagga Wagga, NSW. 8th Australasian Remote Sensing Conference Proceedings. Canberra.

Bierwirth, P.N. (1996). Investigation of airborne gamma-ray images as a rapid mapping tool for soil and land degradation - Wagga Wagga, NSW. AGSO Record 1996/22.

Bowler, J.M., 1983. Lunettes as indices of hydrologic change: a review of Australian evidence Proc. Ro. Soc. Vic. 95/3, pp 147-168.

Chen, X. Y. 2001. The red clay mantle in the Wagga Wagga region, New South Wales: evaluation of an aeolian dust deposit (Yarabee Parna) using methods of soil landscape mapping. Aust. J. Soil Res., 2001, 39, 61–80.

Dickson, B.L., and Scott, K.M., 1998. Recognition of Aeolian soils of the Blayney district, N.S.W.: implications for mineral exploration. Journal of Geochemical Exploration, 63, pp 237-251.

English, P., Richardson, P., Stauffacher, M., 2002. Groundwater & Salinity Processes in Simmons Creek sub-catchment, Billabong Creek, NSW. CSIRO Land and Water, Canberra Technical Report 24/02.

Evans, W.R., 1998. What does Boorowa tell us? Salt stores and groundwater dynamics in a dryland salinity environment. In Weaver TR and Lawrence CR (Editors). Proceedings: International Association of Hydrogeologists International Groundwater Conference: Groundwater: Sustainable Solutions. University of Melbourne, 8-13 February, 1998: 267-274.

Gallant, J.C., and Dowling, T.I., 2003. A multiresolution index of valley bottom flatness. Water Resources Research, Vol., 39, no 12, 1347.

Jones, G., Baker, P., Dent, D., 2003. Billabong Ck interpretation. In MDBC Airborne Geophysics Project: Final Report, Ed: D. Dent. Bureau of Rural Sciences, Consultancy D 2018.

Lane, R., Brodie, R., and Fitzpatrick, A., 2004. Constrained inversion of AEM data from the Lower Balonne area, southern Queensland Australia. CRC LEME open file report. 163 Sept, 2004.

McKenzie, N.J., and Gallant J.C., 2005. Digital soil mapping with improved environmental predictors and models of pedogenesis. In 'Advances in digital soil mapping.' Developments in Soil Science Series (Eds P Lagacherie, AB McBratney, M Voltz), Elsevier.

Melis, M.I., and Acworth, R.I., 2001 An aeolian component in Pleistocene and Holocene valley aggradation: evidence from Dicks Creek catchment, Yass, New South Wales. Aust. J. Soil Res, 39, pp13–38.

Wilford J.R, Dent, D.L., Dowling, T, and Braaten, R, 2001. Rapid mapping of soils and salt stores using airborne radiometrics and digital elevation models. AGSO Research Newsletter, May, 2001, pp33-40